Published in final edited form as:

J Neuroimaging. 2020 July ; 30(4): 428–442. doi:10.1111/jon.12719.

MR Intracranial Vessel Wall Imaging: A Systematic Review

Jae W. Song, MD, MS[1], **Brianna F. Moon, BS**[2], **Morgan P. Burke**[1], **Srikant Kamesh Iyer, PhD**[1], **Mark A. Elliott, PhD**[1], **Haochang Shou, PhD**[3], **Steven R. Messè, MD**[4], **Scott E. Kasner, MD**[4,5], **Laurie A. Loevner, MD**[1,6], **Mitchell D. Schnall, MD, PhD**[1], **John E. Kirsch, PhD**[7], **Walter R. Witschey, PhD**[1,*], **Zhaoyang Fan, PhD**[8,*]

[1]Department of Radiology, University of Pennsylvania, Philadelphia, Pennsylvania, USA

[2]Department of Bioengineering, University of Pennsylvania, Philadelphia, Pennsylvania, USA

[3]Department of Biostatistics, Epidemiology, and Informatics, University of Pennsylvania School of Medicine, USA

[4]Department of Neurology, Hospital of University of Pennsylvania, Philadelphia, Pennsylvania, USA

[5]Department of Emergency Medicine, Hospital of University of Pennsylvania, Philadelphia, Pennsylvania, USA

[6]Department of Otolaryngology, Hospital of University of Pennsylvania, Philadelphia, Pennsylvania, USA

[7]Athinoula A Martinos Center for Biomedical Imaging, Massachusetts General Hospital, Charlestown, Massachusetts, USA

[8]Biomedical Imaging Research Institute, Department of Biomedical Sciences, Cedars-Sinai Medical Center, Los Angeles, California, USA

Abstract

The purpose of this systematic review is to identify trends and extent of variability in intracranial vessel wall MR imaging (VWI) techniques and protocols. Although variability in selection of protocol design and pulse sequence type is known, data on what and how protocols vary is unknown. Three databases were searched to identify publications using intracranial VWI. Publications were screened by predetermined inclusion/exclusion criteria. Technical development publications were scored for completeness of reporting using a modified Nature Reporting Summary Guideline to assess reproducibility. From 2,431 articles, 122 met the inclusion criteria. Trends over the last 23 years (1995–2018) show increased use of 3 Tesla MR ($p<0.001$) and 3D volumetric T1-weighted acquisitions ($p<0.001$). Most (65%) clinical VWI publications report achieving a non-interpolated in-plane spatial resolution of ≤0.55 mm. In the last decade, an increasing number of technical development (n=20) and 7 Tesla (n=12) publications have been published, focused on pulse sequence development, improving cerebrospinal fluid suppression,

Corresponding Author: Jae W. Song, MD, MS, Assistant Professor of Radiology, Division of Neuroradiology, Hospital of the University of Pennsylvania, 3400 Spruce Street, Philadelphia, PA 19104, Tele: 215-349-8023, Fax: 215-662-3283, jae.song@pennmedicine.upenn.edu.

*These authors contributed equally to this work.

scan efficiency, and imaging ex vivo specimen for histologic validation. Mean Reporting Summary Score for the technical development publications was high (0.87, range: 0.63–1.0) indicating strong scientific technical reproducibility. Innovative work continues to emerge to address implementation challenges. Gradual adoption into the research and scientific community was suggested by a shift in the name in the literature from “high resolution MR” to “vessel wall imaging,” specifying diagnostic intent. Insight into current practices and identifying the extent of technical variability in the literature will help direct future clinical and technical efforts to address needs for implementation.

Keywords

vessel wall MR imaging; intracranial atherosclerotic disease; magnetic resonance imaging; vasculopathy

Introduction

Intracranial vessel wall MR imaging (VWI) is a diagnostic imaging technique used to assess and differentiate intracranial vasculopathies.[1] Conventional vessel imaging techniques, such as computed tomography angiography, digital subtraction angiography, and magnetic resonance angiography, show changes in lumen caliber, which are common morphologic changes in many intracranial vasculopathies and can be deemed nonspecific. Additional anatomic information about the vessel wall pathology by VWI can provide specificity to the working diagnosis and has resulted in an increasing number of publications.[2] However, these publications report a wide variety of technical parameters and protocols, making it challenging to summarize the findings and compare the diagnostic technique across publications. Variability exists with the MR scanner (e.g., magnet strength, vendor, coil hardware), pulse sequence technique (e.g., contrast weighting, spatial coverage), and protocol (e.g., protocol lengths, use and timing of contrast).

One reason for the variability is the continued optimization of the technique. Increasing awareness of imaging artifacts and imaging constraints has resulted in a number of publications focused on further improving scan efficiency and minimizing artifacts.[3] However, to facilitate the clinical translation of VWI for diagnostic imaging, consensus about the optimal methodology and reducing the technical variability would help with standardization across institutions and streamline multicenter diagnostic accuracy studies.

While it is known that there is variability in the selection of protocol design and pulse sequence types, data on what and how protocols vary remain unknown. We identify technical trends in intracranial VWI and examine the extent of technical variability. We also review the innovative direction of the VWI community by assessing technical development publications and assess trends in how these technical advances are incorporated into clinical research. Insight into current practices will help direct future clinical and technical efforts to address needs for implementation.

Methods

Search Strategy

This systematic review was conducted in accordance with the Preferred Reporting Items for Systematic Reviews and Meta-Analyses guidelines. PubMed, EMBASE, and Medline were searched on September 12, 2018. To identify eligible studies, keywords covering vessel wall imaging, intracranial circulation, and vasculopathy keywords were searched using the Boolean operators “OR” and “AND” and previously reported in detail (Table 1).[2] A manual review of the citations of each included article was also performed. All foreign language articles were translated. This literature search was previously used to assess vasculopathy type and funding trends of intracranial VWI publications.[2] For this review, the inclusion criteria were modified and publications re-screened to assess protocols and technical trends.

Study selection

Two raters independently reviewed all publications for inclusion with discrepancies resolved by consensus. Inclusion criteria were (a) clinical research or technical development studies; (b) humans; (c) intracranial arteries with or without vasculopathy; (d) magnetic resonance imaging; and (e) vessel wall imaging. Studies with insufficient MR parameter information, single case reports, conference abstracts, and animal studies were excluded.

Data extraction

Data on MR vendor, magnet strength (Tesla, T), head coil, pulse sequence parameters, protocols, spatial resolution, acquisition plane and coverage, year of publication, study type, and studied vasculopathy were collected.

Acquired spatial resolution was calculated from the reported matrix size and field of view. If pulse sequence type (e.g., turbo/fast spin echo (TSE/FSE)) was not reported, the authors identified sequence type based on imaging parameters. Acquisition coverage was described as imaging the whole brain, a vessel segment (e.g., aneurysm, vessel stenosis), or the circle of Willis (e.g., anterior and posterior circulation).

To account for publications that originated from the same investigator/institution, publications were matched by corresponding author and institution. If more than 1 publication was identified from the same corresponding author/institution, MR vendor/protocol data were used from only 1 of the group’s most recent publications to avoid duplicating counts from prolific investigators. Analyses about clinical VWI protocol designs were performed only on clinical research investigations.

Technical development studies were further scored for completeness of reporting based on the MR Acquisition Section of the Nature Reporting Summary guidelines for MR studies[4]; the guideline was modified to include head coil, acquisition time, spatial resolution, and echo train length/turbo factor (Table 2). Sixteen criteria were scored as 1 (complete reporting), 0.5 (partial reporting), or 0 (did not fulfill reporting criteria). Scoring was performed independently by two raters and discrepancies resolved by consensus. Inter-rater agreement was calculated for the two raters.

Statistical Analysis

Categorical variables are expressed in counts and percentages. Continuous variables are presented as means and standard deviations or medians and inter-quartile ranges. Agreement was calculated with an unweighted Cohen's kappa. Logistic and linear regressions were used to test trends of categorical and continuous variables over the years, respectively. The Reporting Summary Score (RSS) was calculated by summing the points of the 16 criteria divided by total possible criteria fulfillment; the RSS ranged from 0 to 1. SPSS v19 (IBM, Chicago, IL) was used for statistical analysis.

Results

Search

From 2,431 articles, 1,635 were screened based on the inclusion/exclusion criteria ($k=0.77$, $p<0.001$) (Figure 1). Qualitative synthesis was conducted on 122 publications ($\kappa=0.95$, $p<0.0001$).

Hardware Variability

To survey frequency of MRs by field strength and vendors, publications were matched by corresponding author/institution and vendor (n=104). Since 2008, a significant increase in the use of 3T for VWI emerged over time ($\beta=5.36$, 95% CI 3.34–7.12, $p<0.001$). By 2018, no VWI publications used 1.5T. Among publications using 3T field strength, the GE platform was the most frequently used (n=32), followed by Siemens (n=26), and Philips (n=23). For 7T, Philips was more commonly used (n=6) followed by Siemens (n=3). Among the studies using 3T, an 8 channel head coil was most frequently used (n=51) followed by 32 channel (n=8),[5–12] 16 channel (n=5),[13–17] 64 channel (n=2),[18,19] 12 channel (n=2),[20,21] 20 channel (n=2),[22,23] custom-designed 36 channel (n=1)[24] and 15 channel (n=1).[25] Head coil was not reported in 8 publications.[26–33] Two studies reported using a "standard head coil"[34] and "loop coil (4 cm diameter)."[35]

Clinical Protocol Design Variability

Protocols from clinical research publications (n=93) varied with different combinations of T1-weighted (T1w), T2-weighted (T2w), and proton density-weighted (PDw) sequences (Figure 2A). The most common VWI protocol included 3D T1w followed by a combination of 2D T1w and 2D T2w acquisitions. Analyses by vasculopathy type showed protocol variability with 3D T1w acquisitions most frequently used to study atherosclerosis and dissection compared to 2D T1w for vasculitis, aneurysm, and reversible cerebral vasoconstriction syndrome (Figure 2B–D).

Most publications (86%) used time-of-flight magnetic resonance angiography (TOF-MRA) as the lumen-based imaging technique. No luminal imaging was reported for 8% of the publications. Both TOF-MRA and contrast-enhanced MRA (CE-MRA) were used in 3% of publications, while 1% reported using CE-MRA only.

The majority of the publications (n=67%) reported including postcontrast imaging among which 34% reported the contrast injection-to-scan time interval. The injection-to-scan time

ranged from “immediate”[36] to “within 20 minutes.”[37] Other publications reported durations of 3 minutes (n=2),[38,39] 4 minutes (n=1)[17], and 5 minutes (n=16).[5,7,14,21,40–51] One publication evaluated only postcontrast without precontrast imaging.[14]

Pulse Sequence Variability

Figure 3 shows the percentages of 2D versus 3D and T1w, T2w, and PDw pulse sequences types. A trend was noted over 23 years with increased use of 3D T1w acquisitions compared to 2D acquisitions (β=2.54, 95% CI 1.29–3.80, $p<0.001$). The most common pulse sequence type was TSE/FSE or variable flip angle turbo spin echo (VFA-TSE; common vendor labels for VFA-TSE are sampling perfection with application optimized contrasts using different flip angle evolution (SPACE) for Siemens, volume isotropic turbo spin echo acquisition (VISTA) or volumetric isotropically reconstructed turbo spin-echo acquisition (VIRTA) for Philips, and CUBE for GE healthcare).

The in-plane spatial resolution varied widely. Among the 82 clinical imaging publications that used T1w acquisitions on 1.5T or 3T, 46 did not report spatial resolutions and 20 reported an interpolation step. True acquired in-plane resolution was calculated by the authors. Twenty-three publications had insufficient parameter details and are not included in this analysis. Most (65%, n=38) publications achieved an in-plane resolution of ≤0.55mm with coverage focused on a vessel segment (n=22), circle of Willis (n=3) or whole brain (n=1) (Figure 4).

Motion and poor quality were cited as reasons for data exclusion in 40% of publications. Fifty-five articles did not report motion as a reason for exclusion, and it is unclear whether all exams were considered good quality or this information was not reported. When reported, a mean of 5% (range: 0–17%) of collected cases were excluded due to motion/poor quality. This loss of data due to motion degradation further highlights the need for improved scan efficiency.

Technical Development on 3T

The evolution of VWI has depended on technical innovations primarily focused on scan efficiency and reducing artifacts (e.g., CSF and blood suppression). Table 3 summarizes the 20 technical development articles at 3T. Study aims include pulse sequence development,[6,52,53] improving scan efficiency,[54–56] CSF suppression,[9,11,57,58] assessment of reliability,[59–63] and comparisons of 2D versus 3D acquisitions,[64,65] acquisition planes,[66] and 3T versus 7T imaging.[22,67]

To assess reporting completeness, a Reporting Summary Score (RSS) was calculated (κ=0.33, $p<0.001$) for the technical development publications. The mean RSS of the 20 publications was 0.87 (range: 0.63 to 1.0), suggesting strong technical reproducibility. Criteria that scored low included reporting the k-space sampling method (mean=0.28), matrix size (mean=0.65), and description of anatomic coverage (mean=0.75).

Ultra-high field 7T VWI

Table 4 summarizes 12 publications using 7T MR. Four publications imaged ex vivo specimens[68–71] with acquisition times ranging from 1 hour 35 minutes to 11 hours 7 minutes. Publications covered topics of feasibility and sequence development,[72–74] histologic validation,[68–71] comparisons of 3T versus 7T[22,75] and examining vasculopathies.[76–78] The most commonly studied intracranial vasculopathies were atherosclerosis and aneurysms.

Clinical Adoption of 3T Technical Developments

Over the last decade, VWI pulse sequence developments have mainly focused on VFA-TSE at 3T. To reduce artifacts, magnetization preparations for blood and CSF suppression have been investigated.[9,11,57,58] The impact of these ongoing improvements to VWI pulse sequences were trended by online publication dates (Figure 5). Online publication dates were used to show precision in chronological trends. After the first publication to use VFA-TSE,[79] an increasing number of clinical publications used VFA-TSE from 2013 onward. Blood suppression magnetization preparation modules were previously used to study carotid vessel wall MR and the results suggest this technique was more readily incorporated into intracranial VWI clinical research investigations. A CSF suppression module was first reported by Wang et al[57] using delay-alternating with nutation for tailored excitation (DANTE, a blood-suppressing magnetization preparation module). A truly dedicated CSF suppression module was subsequently published by Fan et al,[58] after which an increasing number of technical development and clinical imaging publications reported VWI with different CSF suppression techniques.

Trends in Names for VWI

The name for VWI was classified into 3 categories: “vessel wall imaging or high-resolution vessel wall imaging,” “high-resolution MR” and “other.” The name “high-resolution MR” peaked in 2016. A shift was noted in 2017 with more frequent use of the specific term “vessel wall imaging” (Figure 6), indicating diagnostic intent in the name.

Discussion

Considerable technical variability exists for intracranial vessel wall MR imaging. We identified changing trends and most common practices based on the literature. VWI is now primarily performed at 3T with no publications at 1.5T identified in 2018. The selection of pulse sequence and protocol design remains variable. Literature shows a shift from 2D to 3D volumetric acquisitions. There is gradual adoption of technical developments for VWI pulse sequences aimed to reduce blood and CSF flow artifacts. While advancements with technical optimization and innovative research on 7T MR continue, VWI remains clinically investigative and is in the assessment phase of the health technology assessment framework.

The American Society of Neuroradiology Vessel Wall Study Group set forth expert consensus recommendations for techniques to consider.[1] Results show that 3T has become the magnet strength of choice, likely due to a higher signal-to-noise ratio than that available from 1.5T, and most studies achieve the recommended 0.5 mm in-plane spatial resolution.

Results show a 3D T1w sequence to be most commonly used for VWI. However, selection of the optimal combination of tissue weightings for protocol design may vary by vasculopathy type and institutional clinical workflows. The role of 7T MR remains innovative and investigative with studies reporting on feasibility.[22,75]

Several insights from this study warrant attention. First, lengthy acquisition times are a barrier to implementation and is evidenced by the high reported rates of data exclusion due to motion degraded images. This loss of data highlights the need for improved scan efficiency. Second, the American Society of Neuroradiology Vessel Wall study group recommends an in-plane resolution of ≤0.5mm.[1] Although, most publications are achieving this recommended resolution, spatial coverage varied widely. A possible explanation for this may be based on clinical indications. Assessing vasculitis or ICAD may be more diffuse with advantages of imaging the whole-brain with 3D imaging. By contrast, 2D acquisitions and multiple contrast weightings may be optimal to characterize a vessel segment for stenosis or an aneurysm. Indeed, our results show different protocols are reported for different intracranial vasculopathies, highlighting an area for future investigations. Third, wall enhancement signal intensity varies by the contrast injection-to-postcontrast image duration.[80] The wide range of reported injection-to-scan time indicates a need for concerted efforts towards consistency and a need to identify a defined time interval in protocol design. Finally, CSF suppression techniques such as utilizing a post readout magnetization flip-down,[58] anti-driven equilibrium module,[11] or DANTE preparation[57] are being investigated for intracranial VWI. These techniques reportedly reduce vessel wall signal-to-noise ratios leading to underestimations of imaging endpoint metrics, such as vessel wall thickness.[9]

The impact of technical variability for VWI hinges upon identifying reliable imaging endpoints/biomarkers for the type of intracranial vasculopathy being assessed. Questions remain as to which imaging endpoints are the strongest for diagnostic accuracy. To identify endpoints, meaningful data synthesis by meta-analyses requires reduced data heterogeneity. For example, a meta-analysis assessing intracranial atherosclerotic plaque using VWI reported wall enhancement, positive wall remodeling, and plaque surface irregularity to be significantly associated with ischemic stroke.[81] However, the analysis was hampered by data heterogeneity from patient selection and technique. The development of vessel wall phantoms shows effort towards technical standardization across sites.[82] Furthermore, in parallel, assessing diagnostic performance with consensus on imaging endpoints is needed to determine the necessary degree of imaging precision and measurement reliability.[39,59,60,62,63,83] A future direction is to assess the diagnostic performance of imaging endpoints by vasculopathy type. Consensus on which imaging endpoint is critical for diagnosis, defining the minimum clinically achievable image quality, and showing measurement reliability and reproducibility are important steps for generalizability.

Clinical adoption is incremental. It is promising to see gradual incorporation of technical developments into clinical research. In recent years, a shift in the name from “high-resolution MR” to “vessel wall imaging” emerged suggesting universal recognition of the technique specifically for vessel wall assessment. “High-resolution” MR is vague and could reflect spatial or temporal resolution. Thus, the shift to “vessel wall imaging,” conferring diagnostic intent and specificity, is a step towards clinical adoption.

A limitation of this systematic review is the available data of MR technical details. Reporting of MR technical parameters varied widely across clinical journals. This variability may partly be explained by different journals with varying target audiences. Furthermore, a plethora of vendor specific labels adds a layer of jargon. Among the technical development publications, completeness of reporting was high when assessed by a modified version of the Nature Reporting Guideline suggesting reproducibility.

Conclusion

VWI investigations show active involvement at a medical-scientific interface among clinicians and MR physicists working to optimize technical performance to study intracranial vasculopathies. We show data on the extent of variability of intracranial VWI protocols in the literature. Trends in the literature suggest continued optimizations to address implementation challenges through technical development and innovative research. Based on the published literature, collective efforts leading to clinical adoption is on the horizon.

Acknowledgements and Disclosure:

This study was funded by the RSNA Research & Education Foundation, through grant number RSCH1929. The content is solely the responsibility of the authors and does not necessarily represent the official views of the RSNA R&E Foundation. This study was also funded by the Institute for Translational Medicine and Therapeutics/Thomas B. McCabe and Jeannette E. Laws McCabe Fund (JWS) and NIH National Heart, Lung, and Blood Institute R01HL137984 (WRW) and R01HL147355 (ZF).

References

1. Mandell DM, Mossa-Basha M, Qiao Y, et al. Intracranial vessel wall MRI: principles and expert consensus recommendations of the American Society of Neuroradiology. AJNR Am J Neuroradiol 2017;38:218–29. [PubMed: 27469212]
2. Song JW, Guiry SC, Shou H, et al. Qualitative assessment and reporting quality of intracranial vessel wall MR imaging studies: a systematic review. AJNR Am J Neuroradiol 2019;40:2025–32. [PubMed: 31727743]
3. Lindenholz A, van der Kolk AG, Zwanenburg JJ, et al. The use and pitfalls of intracranial vessel wall imaging: how we do it. Radiology 2018;286:12–28. [PubMed: 29261469]
4. Nature research reporting summary, magnetic resonance imaging, acquisition. Nature Research Website. https://www.nature.com/nature-research/editorial-policies/reporting-standards; https://www.nature.com/documents/nr-reporting-summary-flat.pdf. Published 2019.
5. Wu F, Ma Q, Song H, et al. Differential features of culprit intracranial atherosclerotic lesions: A whole-brain vessel wall imaging study in patients with acute ischemic stroke. Journal of the American Heart Association 2018;7.
6. Zhang L, Zhang N, Wu J, et al. High resolution three dimensional intracranial arterial wall imaging at 3 T using T1 weighted SPACE. Magn Reson Imaging 2015;33:1026–34. [PubMed: 26143482]
7. Wu F, Song H, Ma Q, et al. Hyperintense plaque on intracranial vessel wall magnetic resonance imaging as a predictor of artery-to-artery embolic infarction. Stroke 2018;49:905–11. [PubMed: 29540606]
8. Zou X, Chung Y, Zhang L, et al. Middle cerebral artery atherosclerotic plaques in recent small subcortical infarction: a three-dimensional high-resolution MR study. BioMed Res Int 2015;2015:540217. [PubMed: 26539508]
9. Cogswell PM, Siero JCW, Lants SK, et al. Variable impact of CSF flow suppression on quantitative 3.0T intracranial vessel wall measurements: CSF flow suppression in intracranial vessel wall measurements. J Magn Reson Imaging 2018;48:1120–8. [PubMed: 29603829]

10. Matouk CC, Mandell DM, Günel M, et al. Vessel wall magnetic resonance imaging identifies the site of rupture in patients with multiple intracranial aneurysms: proof of principle. Neurosurgery 2013;72:492–6. [PubMed: 23151622]
11. Yang H, Zhang X, Qin Q, et al. Improved cerebrospinal fluid suppression for intracranial vessel wall MRI. J Magn Reson Imaging 2016;44:665–72. [PubMed: 26950926]
12. Bae YJ, Choi BS, Jung C, et al. Differentiation of deep subcortical infarction using high-resolution vessel wall MR imaging of middle cerebral artery. Korean J Radiol 2017;18:964–72. [PubMed: 29089829]
13. Choi JW, Han M, Hong JM, et al. Feasibility of improved motion-sensitized driven-equilibrium (iMSDE) prepared 3D T1-weighted imaging in the diagnosis of vertebrobasilar artery dissection. J Neuroradiol 2018;45:186–91. [PubMed: 29273530]
14. Jang J, Kim T, Hwang E, et al. Assessment of arterial wall enhancement for differentiation of parent artery disease from small artery disease: comparison between histogram analysis and visual analysis on 3-dimensional contrast-enhanced T1-weighted turbo spin echo MR images at 3T. Korean J Radiol 2017;18:383–91. [PubMed: 28246519]
15. Edjlali M, Gentric JC, Régent-Rodriguez C, et al. Does aneurysmal wall enhancement on vessel wall MRI help to distinguish stable from unstable intracranial aneurysms? Stroke 2014;45:3704–6. [PubMed: 25325912]
16. Yu JH, Kwak HS, Chung GH, et al. Association of intraplaque hemorrhage and acute infarction in patients with basilar artery plaque. Stroke 2015;46:2768–72. [PubMed: 26306752]
17. Ryu CW, Jahng GH, Shin HS. Gadolinium enhancement of atherosclerotic plaque in the middle cerebral artery: relation to symptoms and degree of stenosis. AJNR Am J Neuroradiol 2014;35:2306–10. [PubMed: 25012673]
18. Yun SY, Heo YJ, Jeong HW, et al. Spontaneous intracranial vertebral artery dissection with acute ischemic stroke: high-resolution magnetic resonance imaging findings. Neuroradiol J 2018;31:262–9. [PubMed: 29565222]
19. Jung SC, Kim HS, Choi C-, et al. Spontaneous and unruptured chronic intracranial artery dissection: high-resolution magnetic resonance imaging findings. Clin Neuroradiol 2018;28:171–81. [PubMed: 27677627]
20. Niu PP, Yu Y, Zhou HW, et al. Vessel wall differences between middle cerebral artery and basilar artery plaques on magnetic resonance imaging. Sci Rep 2016;6:38534. [PubMed: 27917937]
21. Omodaka S, Endo H, Niizuma K, et al. Quantitative assessment of circumferential enhancement along the wall of cerebral aneurysms using MR imaging. AJNR Am J Neuroradiol 2016;37:1262–6. [PubMed: 26939634]
22. Zhu C, Haraldsson H, Tian B, et al. High resolution imaging of the intracranial vessel wall at 3 and 7 T using 3D fast spin echo MRI. MAGMA 2016;29:559–70. [PubMed: 26946509]
23. Obusez EC, Hui F, Hajj-Ali R, et al. High-resolution MRI vessel wall imaging: spatial and temporal patterns of reversible cerebral vasoconstriction syndrome and central nervous system vasculitis. AJNR Am J Neuroradiol 2014;35:1527–32. [PubMed: 24722305]
24. Chen Z, Liu AF, Chen H, et al. Evaluation of basilar artery atherosclerotic plaque distribution by 3D MR vessel wall imaging. J Magn Reson Imaging 2016;44:1592–9. [PubMed: 27249041]
25. Sun L, Li Z, Tang W, et al. High resolution magnetic resonance imaging in pathogenesis diagnosis of single lenticulostriate infarction with nonstenotic middle cerebral artery, a retrospective study. BMC Neurol 2018;18.
26. Ahn SH, Lee J, Kim YJ, et al. Isolated MCA disease in patients without significant atherosclerotic risk factors: a high-resolution magnetic resonance imaging study. Stroke 2015;46:697–703. [PubMed: 25628303]
27. Thaler C, Kaufmann-Bühler A, Gansukh T, et al. Neuroradiologic characteristics of primary angiitis of the central nervous system according to the affected vessel size. Clin Neuroradiol 2019;29:37–44. [PubMed: 28875326]
28. Li F, Chen QX, Chen ZB, et al. Magnetic resonance imaging of plaque burden in vascular walls of the middle cerebral artery correlates with cerebral infarction. Curr Neurovasc Res 2016;13:263–70. [PubMed: 27573442]

29. Chen CY, Chen SP, Fuh JL, et al. Vascular wall imaging in reversible cerebral vasoconstriction syndrome - A 3-T contrast-enhanced MRI study. J Headache Pain 2018;19. [PubMed: 29500688]
30. Muraoka S, Araki Y, Taoka T, et al. Prediction of intracranial arterial stenosis progression in patients with moyamoya vasculopathy: contrast-enhanced high-resolution magnetic resonance vessel wall imaging. World Neurosurg 2018;116:e1114–21. [PubMed: 29864569]
31. Cheng-Ching E, Jones S, Hui FK, et al. High-resolution MRI vessel wall imaging in varicella zoster virus vasculopathy. J Neurol Sci 2015;351:168–73. [PubMed: 25732801]
32. Niizuma K, Shimizu H, Takada S, et al. Middle cerebral artery plaque imaging using 3-Tesla high-resolution MRI. J Clin Neurosci 2008;15:1137–41. [PubMed: 18703337]
33. Feng C, Xu Y, Bai X, et al. Basilar artery atherosclerosis and hypertensive small vessel disease in isolated pontine infarctions: A study based on high-resolution MRI. Eur Neurol 2013;70:16–21. [PubMed: 23652613]
34. Mossa-Basha M, Shibata DK, Hallam DK, et al. Added value of vessel wall magnetic resonance imaging for differentiation of nonocclusive intracranial vasculopathies. Stroke 2017;48:3026–33. [PubMed: 29030476]
35. Jiang Y, Zhu C, Peng W, et al. Ex-vivo imaging and plaque type classification of intracranial atherosclerotic plaque using high resolution MRI. Atherosclerosis 2016;249:10–6. [PubMed: 27062404]
36. Skarpathiotakis M, Mandell DM, Swartz RH, et al. Intracranial atherosclerotic plaque enhancement in patients with ischemic stroke. AJNR Am J Neuroradiol 2013;34:299–304. [PubMed: 22859280]
37. Vakil P, Vranic J, Hurley MC, et al. T1 gadolinium enhancement of intracranial atherosclerotic plaques associated with symptomatic ischemic presentations. AJNR Am J Neuroradiol 2013;34:2252–8. [PubMed: 23828109]
38. Huang B, Yang WQ, Liu XT, et al. Basilar artery atherosclerotic plaques distribution in symptomatic patients: A 3.0 T high-resolution MRI study. Eur J Radiol 2013;82:e199–203. [PubMed: 23228280]
39. Yang W, Huang B, Liu X, et al. Reproducibility of high-resolution MRI for the middle cerebral artery plaque at 3T. Eur J Radiol 2014;83:49.
40. Wang M, Yang Y, Zhou F, et al. The contrast enhancement of intracranial arterial wall on high-resolution MRI and its clinical relevance in patients with moyamoya vasculopathy. Sci Rep 2017;7.
41. Lou X, Jiang W, Ma L, et al. In vivo high-resolution magnetic resonance imaging in severe intracranial stenosis. Zhonghua Nei Ke Za Zhi 2008;47:478–81. [PubMed: 19040065]
42. Lou X, Ma N, Ma L, et al. Contrast-enhanced 3T high-resolution MR imaging in symptomatic atherosclerotic basilar artery stenosis. AJNR Am J Neuroradiol 2013;34:513–7. [PubMed: 22878005]
43. Harteveld AA, van der Kolk AG, van der Worp HB, et al. Detecting intracranial vessel wall lesions with 7T-magnetic resonance imaging: patients with posterior circulation ischemia versus healthy controls. Stroke 2017;48:2601–4. [PubMed: 28701579]
44. Qiao Y, Anwar Z, Intrapiromkul J, et al. Patterns and implications of intracranial arterial remodeling in stroke patients. Stroke 2016;47:434–40. [PubMed: 26742795]
45. Klein IF, Lavallée PC, Touboul PJ, et al. In vivo middle cerebral artery plaque imaging by high-resolution MRI. Neurology 2006;67:327–9. [PubMed: 16864831]
46. Qiao Y, Zeiler SR, Mirbagheri S, et al. Intracranial plaque enhancement in patients with cerebrovascular events on high-spatial-resolution MR images. Radiology 2014;271:534–42. [PubMed: 24475850]
47. Wang Y, Lou X, Li Y, et al. Imaging investigation of intracranial arterial dissecting aneurysms by using 3 T high-resolution MRI and DSA: From the interventional neuroradiologists' view. Acta Neurochir 2014;156:515–25. [PubMed: 24420008]
48. Jiang W, Yu W, Ma N, et al. High resolution MRI guided endovascular intervention of basilar artery disease. J NeuroInterv Surg 2011;3:375–8. [PubMed: 21990448]

49. van der Kolk AG, Zwanenburg JJM, Brundel M, et al. Distribution and natural course of intracranial vessel wall lesions in patients with ischemic stroke or TIA at 7.0 tesla MRI. Eur Radiol 2015;25:1692–700. [PubMed: 25577517]
50. Kim TH, Choi JW, Roh HG, et al. Atherosclerotic arterial wall change of non-stenotic intracracranial arteries on high-resolution MRI at 3.0 T: Correlation with cerebrovascular risk factors and white matter hyperintensity. Clin Neurol Neurosurg 2014;126:1–6. [PubMed: 25190670]
51. Xu X, Wei Y, Zhang X, et al. Value of higher-resolution MRI in assessing middle cerebral atherosclerosis and predicting capsular warning syndrome. J Magn Reson Imaging 2016;44:1277–83. [PubMed: 27080075]
52. Lou X, Ma N, Shen H, et al. Noninvasive visualization of the basilar artery wall and branch ostia with high-resolution three-dimensional black-blood sequence at 3 Tesla. J Magn Reson Imaging 2014;39:911–6. [PubMed: 24783241]
53. Li M, Xu Y, Hou B, et al. High-resolution intracranial vessel wall imaging using 3D CUBE T1 weighted sequence. Eur J Radiol 2016;85:803–7. [PubMed: 26971427]
54. Lindenholz A, Harteveld AA, Zwanenburg JJ, et al. Comparison of 3T intracranial vessel wall MRI sequences. AJNR Am J Neuroradiol 2018;39:1112–20. [PubMed: 29674412]
55. Zhu C, Tian B, Feng L, et al. Accelerated whole brain intracranial vessel wall imaging using black blood fast spin echo with compressed sensing (CS-SPACE). MAGMA 2018;31:457–67. [PubMed: 29209856]
56. Yang Q, Deng Z, Bi X, et al. Whole-brain vessel wall MRI: a parameter tune-up solution to improve the scan efficiency of three-dimensional variable flip-angle turbo spin-echo. J Magn Reson Imaging 2017;46:751–7. [PubMed: 28106936]
57. Wang J, Helle M, Zhou Z, Börnert P, Hatsukami TS, Yuan C. Joint blood and cerebrospinal fluid suppression for intracranial vessel wall MRI. Magn Reson Med 2016;75:831–8. [PubMed: 25772551]
58. Fan Z, Yang Q, Deng Z, et al. Whole-brain intracranial vessel wall imaging at 3 Tesla using cerebrospinal fluid-attenuated T1-weighted 3D turbo spin echo. Magn Reson Med 2017;77:1142–50. [PubMed: 26923198]
59. Qiao Y, Guallar E, Suri FK, et al. MR imaging measures of intracranial atherosclerosis in a population-based study. Radiology 2016;280:860–8. [PubMed: 27022858]
60. Ma N, Lou X, Zhao T, et al. Intraobserver and interobserver variability for measuring the wall area of the basilar artery at the level of the trigeminal ganglion on high-resolution MR images. AJNR Am J Neuroradiol 2011;32:E29–32. [PubMed: 20223883]
61. Yang W, Huang B, Liu X, Liu H, Li P, Zhu W. Reproducibility of high-resolution MRI for the middle cerebral artery plaque at 3T. Eur J Radiol 2014;83:49.
62. Zhang X, Zhu C, Peng W, et al. Scan-rescan reproducibility of high resolution magnetic resonance imaging of atherosclerotic plaque in the middle cerebral artery. PLoS ONE 2015;10.
63. Zhang N, Zhang F, Deng Z, et al. 3D whole-brain vessel wall cardiovascular magnetic resonance imaging: a study on the reliability in the quantification of intracranial vessel dimensions. J Cardiovasc Magn Reson 2018;20:39-z. [PubMed: 29898736]
64. Choi JW, Han M, Hong JM, et al. Feasibility of improved motion-sensitized driven-equilibrium (iMSDE) prepared 3D iation of assoT1-weighted imaging in the diagnosis of vertebrobasilar artery dissection. J Neuroradiol 2018;45:186–91. [PubMed: 29273530]
65. Qiao Y, Steinman DA, Qin Q, et al. Intracranial arterial wall imaging using three-dimensional high isotropic resolution black blood MRI at 3.0 Tesla. J Magn Reson Imaging 2011;34:22–30. [PubMed: 21698704]
66. Dieleman N, Yang W, van der Kolk AG, et al. Qualitative evaluation of a high-resolution 3D multi-sequence intracranial vessel wall protocol at 3 Tesla MRI. PloS One 2016;11:e0160781. [PubMed: 27532106]
67. Harteveld AA, van der Kolk AG, van der Worp HB, et al. High-resolution intracranial vessel wall MRI in an elderly asymptomatic population: comparison of 3T and 7T. Eur Radiol 2017;27:1585–95. [PubMed: 27387876]

68. Majidi S, Sein J, Watanabe M, et al. Intracranial-derived atherosclerosis assessment: an in vitro comparison between virtual histology by intravascular ultrasonography, 7T MRI, and histopathologic findings. AJNR Am J Neuroradiol 2013;34:2259–64. [PubMed: 23811977]
69. Kleinloog R, Korkmaz E, Zwanenburg JJ, et al. Visualization of the aneurysm wall: a 7.0-Tesla magnetic resonance imaging study. Neurosurgery 2014;75:614–22. [PubMed: 25255252]
70. Harteveld AA, Denswil NP, Van Hecke W, et al. Ex vivo vessel wall thickness measurements of the human circle of Willis using 7T MRI. Atherosclerosis 2018;273:106–14. [PubMed: 29715587]
71. Harteveld AA, Denswil NP, Siero JC, et al. Quantitative intracranial atherosclerotic plaque characterization at 7T MRI: an ex vivo study with histologic validation. AJNR Am J Neuroradiol 2016;37:802–10. [PubMed: 26705320]
72. Viessmann O, Li L, Benjamin P, et al. T2-weighted intracranial vessel wall imaging at 7 Tesla using a DANTE-prepared variable flip angle turbo spin echo readout (DANTE-SPACE). Magn Reson Med 2017;77:655–63. [PubMed: 26890988]
73. van der Kolk AG, Zwanenburg JJ, Brundel M, et al. Intracranial vessel wall imaging at 7.0-T MRI. Stroke 2011;42:2478–84. [PubMed: 21757674]
74. van der Kolk AG, Hendrikse J, Brundel M, et al. Multi-sequence whole-brain intracranial vessel wall imaging at 7.0 tesla. Eur Radiol 2013;23:2996–3004. [PubMed: 23736375]
75. Harteveld AA, van der Kolk AG, van der Worp HB, et al. Detecting intracranial vessel wall lesions with 7T-magnetic resonance imaging: patients with posterior circulation ischemia versus healthy controls. Stroke 2017;48:2601–4. [PubMed: 28701579]
76. van der Kolk AG, Zwanenburg JJM, Brundel M, et al. Distribution and natural course of intracranial vessel wall lesions in patients with ischemic stroke or TIA at 7.0 tesla MRI. Eur Radiol 2015;25:1692–700. [PubMed: 25577517]
77. Blankena R, Kleinloog R, Verweij BH, et al. Thinner regions of intracranial aneurysm wall correlate with regions of higher wall shear stress: a 7T MRI study. AJNR Am J Neuroradiol 2016;37:1310–7. [PubMed: 26892986]
78. Harteveld AA, van der Kolk AG, van der Worp HB, et al. Detecting intracranial vessel wall lesions with 7T-magnetic resonance imaging: patients with posterior circulation ischemia versus healthy controls. Stroke 2017;48:2601–4. [PubMed: 28701579]
79. Qiao Y, Steinman DA, Qin Q, et al. Intracranial arterial wall imaging using three-dimensional high isotropic resolution black blood MRI at 3.0 tesla. J Magn Reson Imaging 2011;34:22–30. [PubMed: 21698704]
80. de Havenon A, Muhina HJ, Parker DL, et al. Effect of time elapsed since gadolinium administration on atherosclerotic plaque enhancement in clinical vessel wall MR imaging studies. AJNR Am J Neuroradiol 2019;40:1709–11. [PubMed: 31515211]
81. Lee HN, Ryu CW, Yun SJ. Vessel-wall magnetic resonance imaging of intracranial atherosclerotic plaque and ischemic stroke: a systematic review and meta-analysis. Front Neurol 2018;9:1032. [PubMed: 30559708]
82. Chueh JY, van der Marel K, Gounis MJ, et al. Development of a high resolution MRI intracranial atherosclerosis imaging phantom. J Neurointerv Surg 2018;10:143–9. [PubMed: 28280114]
83. Mossa-Basha M, Watase H, Sun J, et al. Inter-rater and scan-rescan reproducibility of the detection of intracranial atherosclerosis on contrast-enhanced 3D vessel wall MRI. Br J Radiol 2019;92:20180973. [PubMed: 30789784]

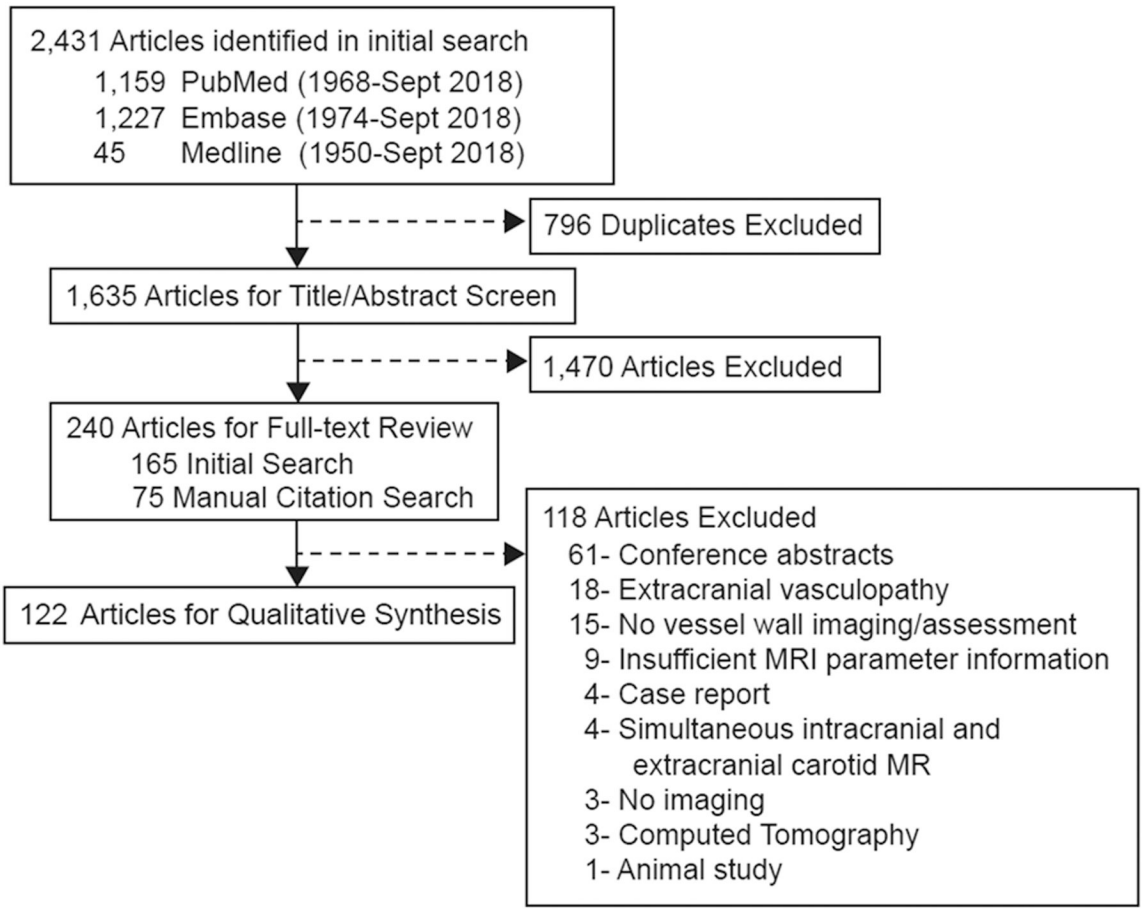

Figure 1: Literature search flowchart.

Database searches from PubMed, EMBASE and Medline identified 2,431 publications. From the initial search, 165 publications were identified for full-text review. A manual review of the citations of the 165 articles identified 807 citations, among which 75 publications met the inclusion/exclusion criteria. A total of 122 publications underwent qualitative data extraction.

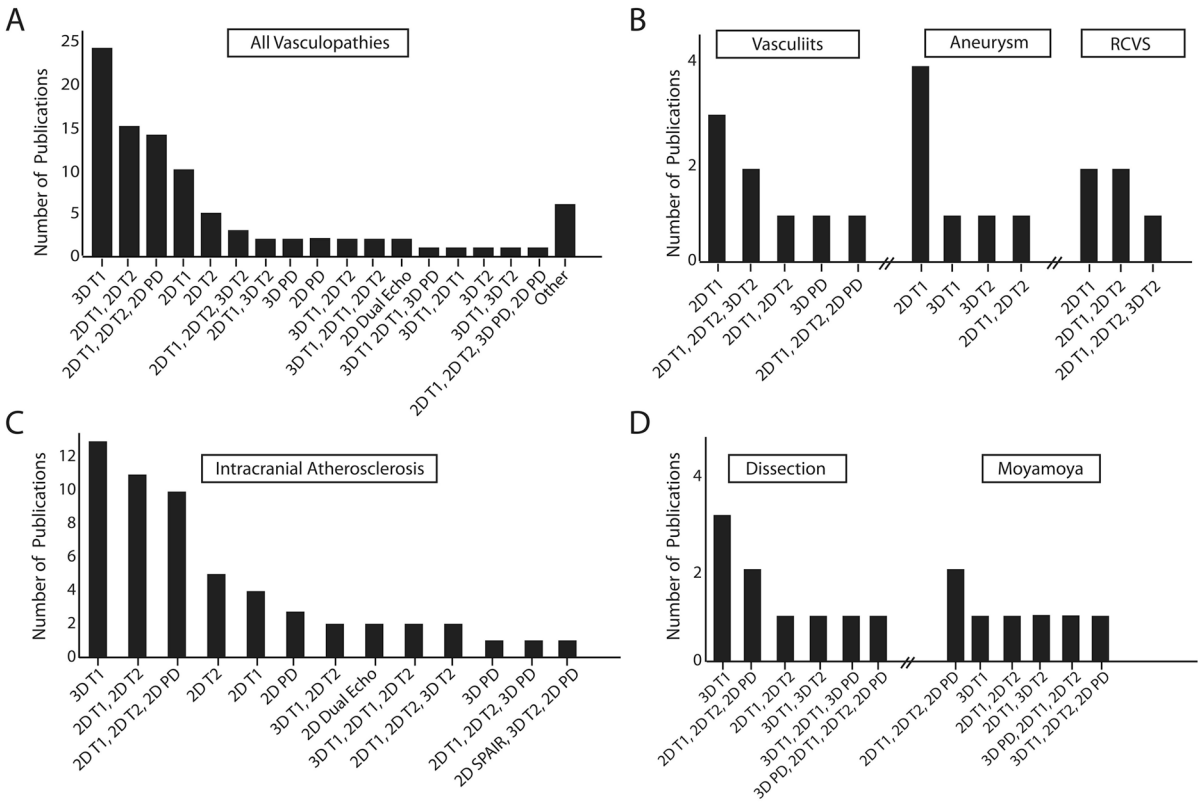

Figure 2: Intracranial vessel wall imaging (VWI) clinical protocol designs.

A: Protocols from 93 clinical publications using 1.5- or 3-Tesla varied with different combinations of T1-weighted (T1w), T2-weighted (T2w), and proton density-weighted (PDw) sequences. B: For intracranial atherosclerosis, 3D T1w acquisitions were the most common VWI protocol design. C: For vasculitis, aneurysms, and reversible cerebral vasoconstriction syndrome (RCVS), 2D T1w acquisitions were the most common protocol design. D: For arterial dissection, a 3D T1w acquisition protocol design was most common. Multicontrast weighting with 2D T1w, 2D T2w, and 2D PDw acquisitions was most commonly used for moyamoya syndrome and disease.

Abbreviation: SPAIR, spectral attenuated inversion recovery.

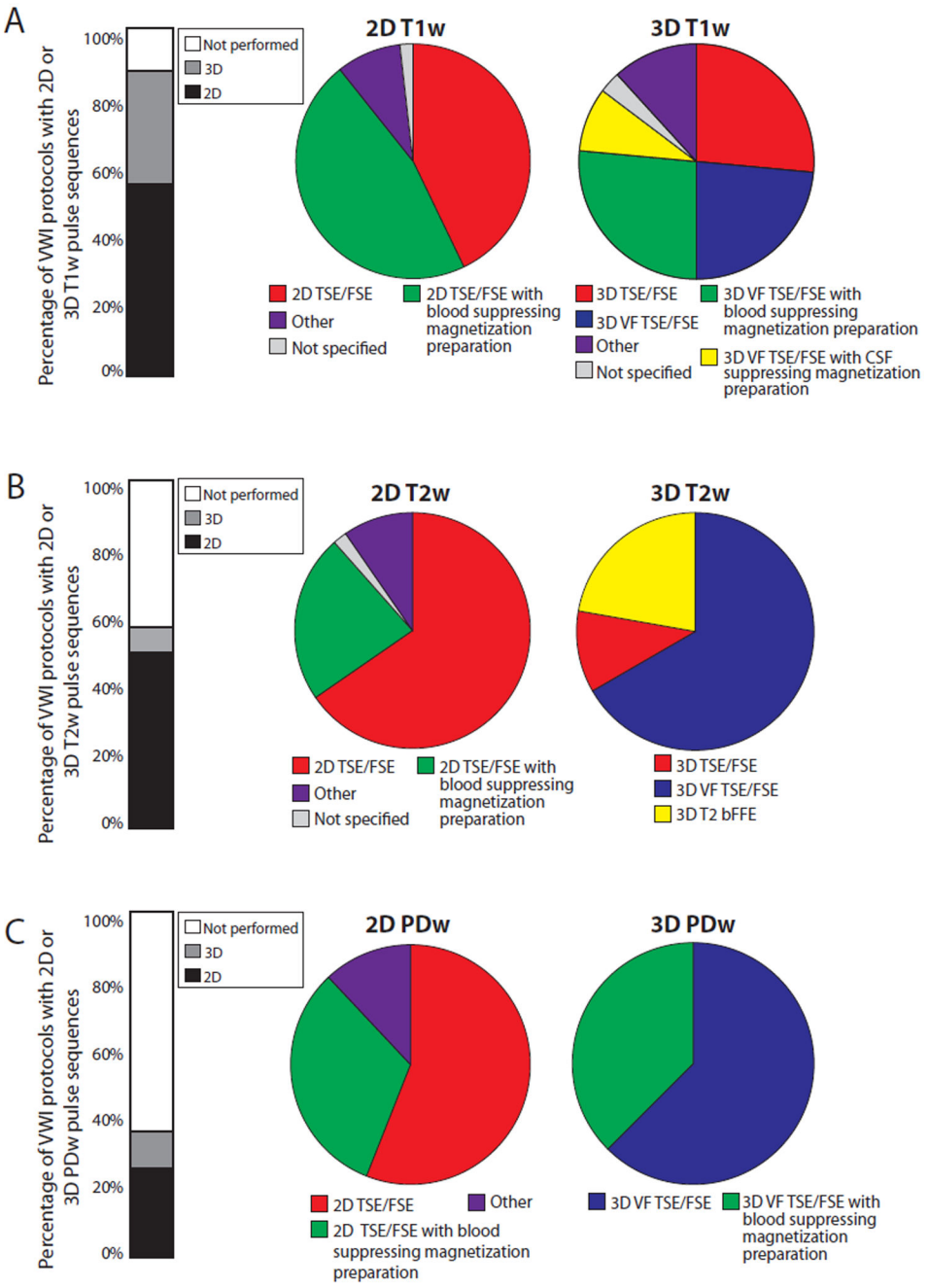

Figure 3: Types of pulse sequences in intracranial vessel wall imaging protocols.

A: Types of T1-weighted (T1w) pulse sequences by 2D and 3D imaging. Other 2D T1w pulse sequences include: T1w fluid-attenuated inversion recovery with (n=1) and without (n=2) blood suppressing magnetization preparation, T1w spin echo with (n=1) and without (n=1) blood suppressing magnetization preparation. Other 3D T1w pulse sequences include: 3D magnetization prepared-rapid gradient echo, phase sensitive inversion recovery enabled 3D inversion recovery turbo field echo, and 3D TSE/FSE with blood suppressing magnetization preparation.

B: Types of T2-weighted (T2w) pulse sequences by 2D and 3D imaging. Other 2D T2w pulse sequences include: T2w spin echo with blood suppressing magnetization preparation (n=1) and dual echo with (n=2) and without (n=1) blood suppressing magnetization preparation. C: Types of proton density-weighted (PDw) pulse sequences by on 2D and 3D imaging. Other 2D PDw pulse sequences include: PDw spin echo (n=1) and dual echo with (n=2) and without (n=1) blood suppressing magnetization preparation.
Abbreviations: VFA-TSE, variable flip angle turbo spin-echo (vendor labels: SPACE, CUBE, VISTA, VIRTA); bFFE, balanced fast field echo.

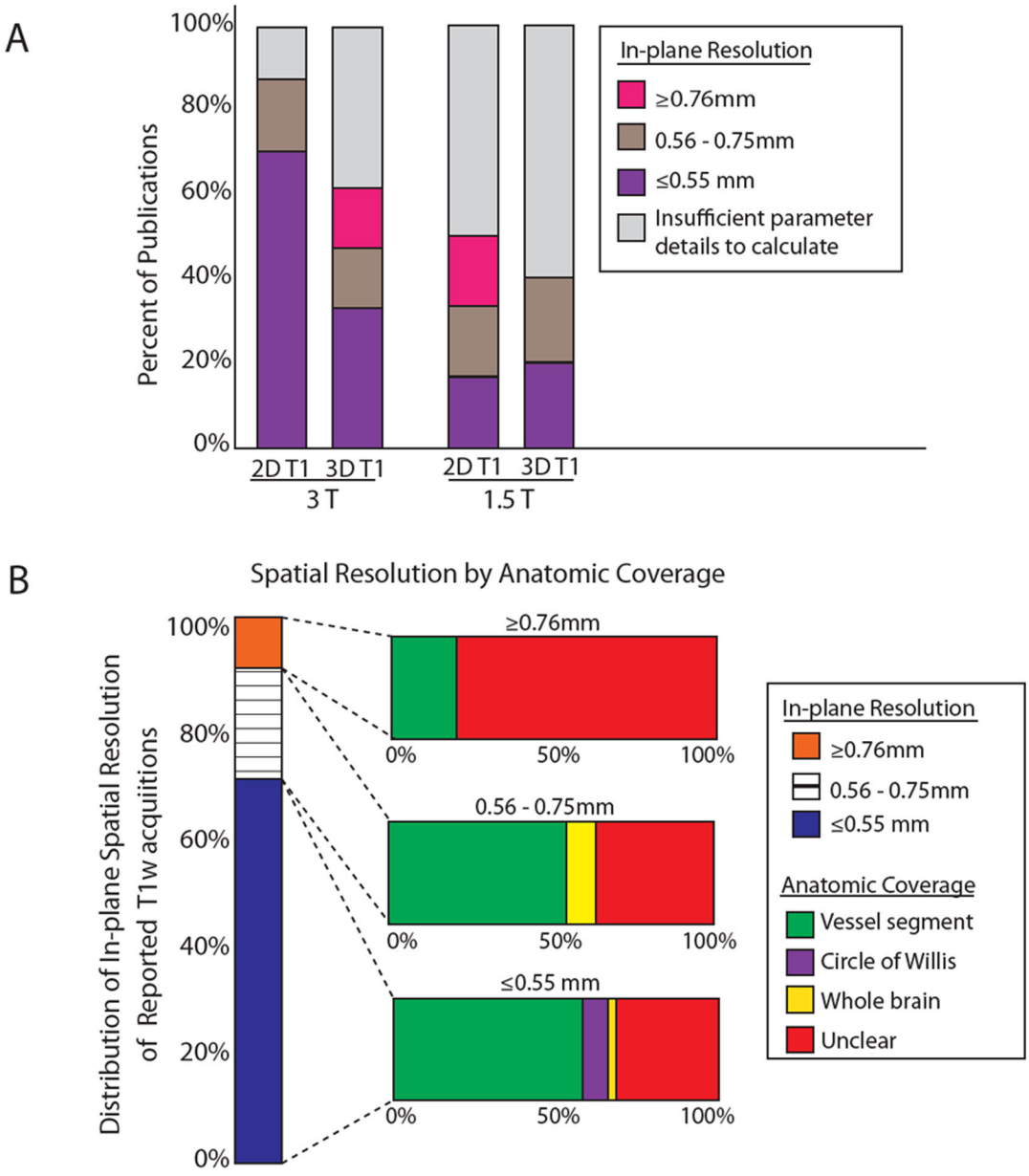

Figure 4: In-plane spatial resolution and anatomic coverage in intracranial vessel wall imaging.
A: Acquired in-plane spatial resolution by magnet field strength. Publications from which non-interpolated spatial resolutions could be calculated were included in this analysis. The distribution of 2D and 3D T1-weighted acquisitions and the calculated in-plane spatial resolution are shown at 3 and 1.5 Tesla. B: Acquired in-plane spatial resolution by imaged anatomic coverage. The distribution of publications using T1-weighted acquisitions by calculated in-plane spatial resolution and imaged anatomic coverage is shown.

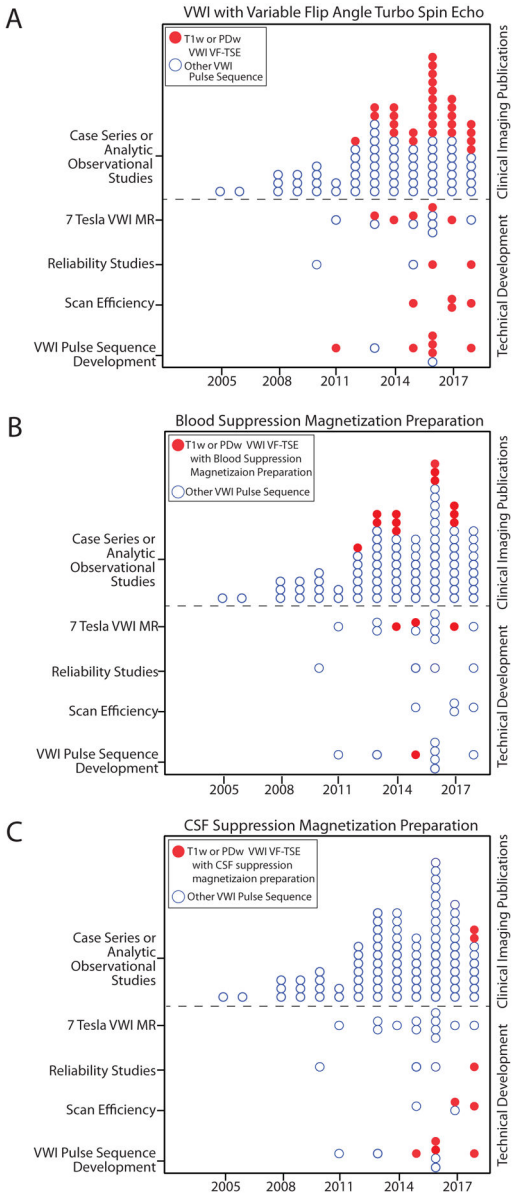

Figure 5: Impact of 3-Tesla technical developments into clinical imaging publications.

A: After the first technical development publication reported the use of VFA-TSE in 2011, an increasing number of publications using this pulse sequence emerged. This transition suggests an adoption of this pulse sequence for clinical vessel wall imaging (VWI) research investigating intracranial vasculopathies. B: Use of blood suppression magnetization preparation modules in clinical imaging publications for intracranial vasculopathies was first seen in 2012 with one dedicated technical development publication testing this module. C: CSF-suppression magnetization preparation was first tested in 2 technical development publications in 2015. A gradual increase in the number of publications in both technical development and clinical imaging publications are seen thereafter.

Abbreviations: VFA-TSE, variable flip angle turbo spin echo; T1w, T1-weighted; PDw, proton density-weighted.

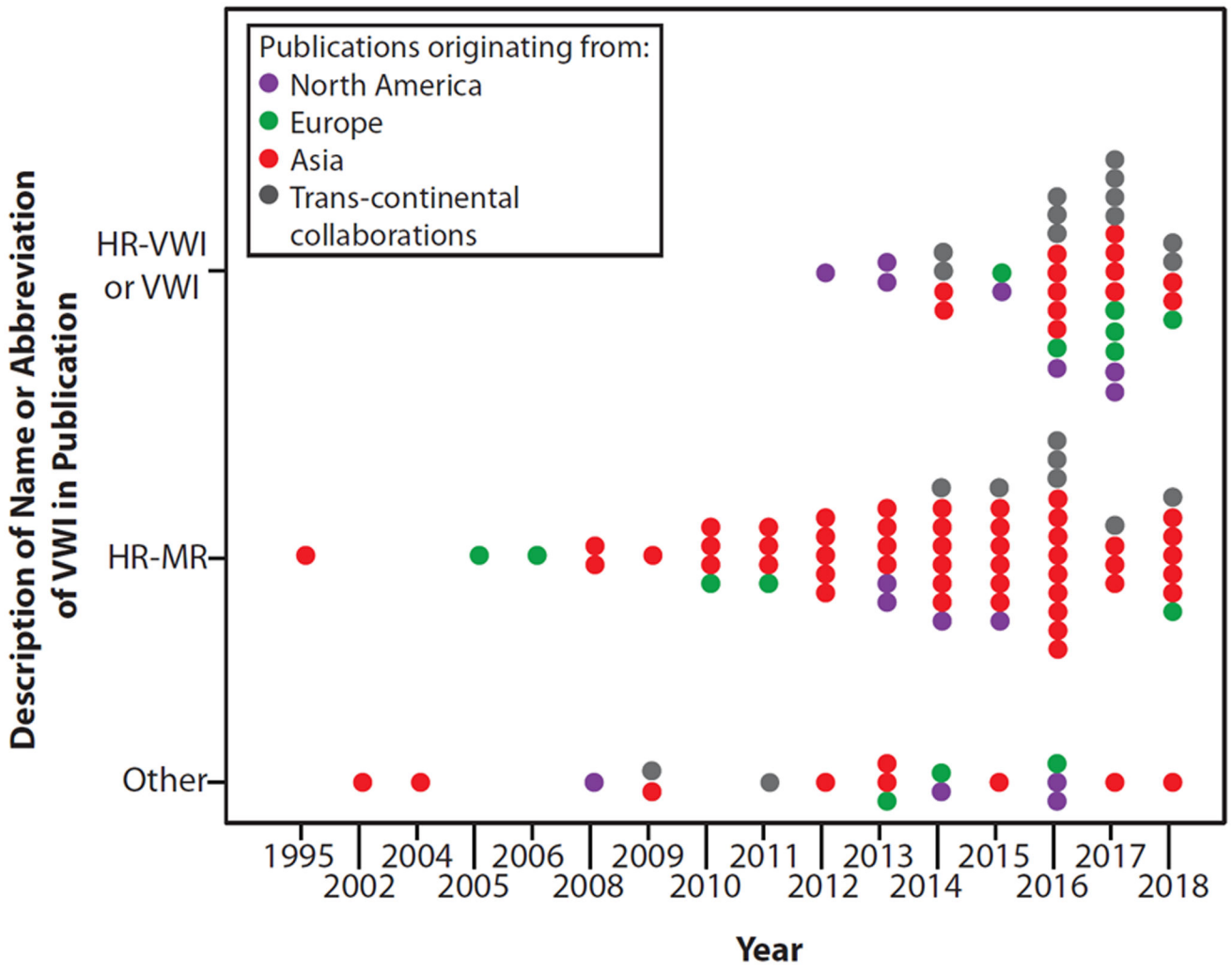

Figure 6:
Changing trends in the name for intracranial vessel wall imaging publications from 1995 to 2018 show a shift in the name in 2016–2017.

Table 1:

Example Search Terms[†]

For Imaging, Key Words Included:
“magnetic resonance imaging” [MeSH Terms] OR (“magnetic”[All Fields] AND “resonance” [All Fields] AND “imaging”[All Fields]) OR “magnetic resonance imaging” [All Fields] OR “mri” [All Fields] OR neuroimaging [MeSH Terms] OR “neuroimaging” [All Fields]
AND
For Vessel Wall MR Imaging, Key Words Included:
“blood vessels” [MeSH Terms] OR “blood”[All Fields] AND “vessels” [All Fields] OR “blood vessels” [All Fields] OR “vessel” [All Fields] AND wall[All Fields] AND “imaging” [All Fields] AND “blood vessels” [MeSH Terms]
AND
For Intracranial Circulation, Key Words Included:
“cerebral arteries” [MeSH Terms] OR (“cerebral” [All Fields] AND “arteries”[All Fields]) OR “cerebral arteries” [All Fields] OR (“cerebral”[All Fields] AND “artery” [All Fields]) OR “cerebral artery” [All Fields], circle of willis [MeSH Terms] OR “circle” [All Fields] AND “willis” [All Fields] OR “circle of willis” [All Fields]
AND
Intracranial vascular disease, Key Words Included:
“cerebral arterial diseases” [MeSH Terms] OR (“cerebral”[All Fields] AND “arterial” [All Fields] AND “diseases” [All Fields]) OR “cerebral arterial diseases” [All Fields] OR (“cerebral” [All Fields] AND “arterial”[All Fields] AND “disease” [All Fields]) OR “cerebral arterial disease” [All Fields], cerebrovascular disorders [MeSH Terms] OR (“cerebrovascular” [All Fields] AND “disorders” [All Fields]) OR “cerebrovascular disorders” [All Fields]

Abbreviations: MeSH, medical subject heading

[†]Complete search terms available in Song et al 2019.[3]

Table 2:

Nature Reporting Summary for Magnetic Resonance Imaging, Acquisition

Nature Reporting Summary Criteria for MR Acquisition[4]	
Imaging type	Specify: functional, structural, diffusion, perfusion
Field strength	Specify in Tesla
Sequence and imaging parameters	Pulse sequence type
	Imaging type
	Field of view
	Matrix size
	Slice thickness
	Plane or orientation of acquisition
	Echo time
	Repetition time
	Flip angle
Area of acquisition	State whether a whole brain scan was used OR define the area of acquisition, describing how the region was determined
Additional vessel wall MR imaging relevant acquisition parameter details	
Acquisition time	
In-plane spatial resolution	
Echo train length or turbo factor	
Head coil	

Table 3:

3T Intracranial Vessel Wall MR Technical Development Publications and Reporting Summary Score

Study*	MR Vendor, Magnet Strength, Head Coil	Study Aim	Protocol	In-plane spatial resolution (reported)	Anatomic Coverage	Acquisition Time	RSS‖
Ma N, et al., 2011.[37]	GE Signa, TwinSpeed, 3T, 8ch	Intra-rater and inter-rater reliability	2D T1w DIR FSE, 2D PDw FSE and 2D T2w FSE	2D T1w: 0.6 ×0.5 mm 2D PDw: 0.6 × 0.5 mm 2D T2w: 0.6 × 0.5 mm	Basilar artery	NR	0.78
Qiao Y, et al., 2011.[41]	Philips, Achieva, 3T, 8ch	Compare sequences (3D PD VISTA and 2D TSE)	3D VISTA, 2D DIR TSE, 3D FLAIR VISTA	3D VISTA: 0.5 mm and 0.4 mm 2D DIR TSE: 0.25 mm and 0.5 mm 3D FLAIR VISTA: 0.5 mm	3D VISTA: coronal, COW// 2D DIR TSE: basilar artery, M1 Middle cerebral artery, petrous ICA 3D FLAIR VISTA: NR	3D VISTA: 7.9 min & 7.6 min 2D DIR TSE: 74 secs/slice & 37 secs/slice 3D FLAIR VISTA: NR	0.94
Yang WQ, et al., 2014.[8]	GE Signa Excite HD, 3T, 8ch	Intra-rater and inter-rater reproducibility	2D DIR T1w FSE, 2D T2w	T1w: 0.51 mm T2w: 0.51 mm	Middle cerebral artery	NR	0.72
Lou X, et al., 2014.[26]	GE Signa, Twin Speed, 3T, 8ch	Test sequence	3D FDP-FSPGR	0.6 × 0.5 mm	Basilar artery	239 secs	0.79
Wang J, et al., 2016.[35]	Philips, Achieva, 3T, 8ch	CSF and blood suppression (DANTE pre-pulse)	PDw VF-TSE with and without DANTE	0.6 mm	NR§§	5 min 29 secs	0.81
Zhang L, et al., 2015.[27]	Siemens, Trio, 3T, 32ch	Test sequence (3D T1w VF-TSE)	T1w VF-TSE	Two T1w SPACE pulse sequences: 0.52 mm & 0.5 mm	Middle cerebral artery, basilar artery, petrous ICA	10 min	0.91
Zhang X, et al., 2015.[38]	GE Signa 3.0T HDxt, 8ch	Scan-rescan reproducibility	2D T2w FSE	0.39 × 0.31 mm	Middle cerebral artery	3 min 45 sec	0.88
Li ML, et al., 2016.[28]	GE Discovery, MR750, 3T, 8ch	Test sequence (3D VF-TSE)	T2w†, 3D T1w VF-TSE	0.64 mm (calculated acquired) 0.4 mm (reconstructed)	COW††	5 min	0.85
Fan Z, et al., 2017.[33]	Siemens, Verio, 3T, 32ch	CSF suppression and increase spatial coverage to whole brain	3D T1w VF-TSE and 3D T1w IR VF-TSE	0.52 mm	Whole brain	11 min 14 secs to 12 min	0.94
Zhu C, et al., 2016.[43]	Siemens Skyra, 3T, 20ch	Compare 3T and 7T MR‡	3T: 3D VF-TSE with ETL40 and ETL60	3T: 3D VF-TSE with ETL40 and ELT60: 0.5 mm	COW‡‡	3T: 3D VF-TSE with ETL40: 10 min 14 secs 3D VF-TSE with ETL60: 9 min 58 secs	0.94
Yang H et al., 2016.[34]	Philips, Achieva, 3T, 32ch	Optimize CSF suppression (anti-DRIVE)	3D T1w VF-TSE with anti-DRIVE§	0.5 mm	NR	5.4 min	0.88

Study*	MR Vendor, Magnet Strength, Head Coil	Study Aim	Protocol	In-plane spatial resolution (reported)	Anatomic Coverage	Acquisition Time	RSS//
Qiao Y, et al., 2016.[36]	Multi-site study**, Siemens, 3T	Scan-rescan, intra-rater, inte-rrater reliability	3D VF-TSE	0.5 mm	COW	8.3 min	0.94
Harteveld AA, et al., 2017.[44]	Philips Achieva, 3T, 8ch	Compare 3T and 7T MR≠	3T: 3D T1w VIRTA with anti-DRIVE	3T: 0.6 mm (acquired); 0.5 mm (reconstructed)	3T: COW	3T: 6 min 51 secs	0.88
Dieleman, N, et al., 2016.[42]	Philips, Achieva, 3T, 8ch	Compare contrast weighting and acquisition planes	T1w VIRTA transverse with anti-driven Equilibrium (DRIVE) module and T1w/T2w/PDw VIRTA sagittal;	T1w VIRTA transverse and sagittal: 0.6 mm (acquired), 0.5 mm (reconstructed) T2w VIRTA sagittal: 0.7 mm (acquired), 0.6 mm (reconstructed) PDw VIRTA sagittal: 0.6 mm (acquired), 0.3 mm (reconstructed)	COW	T1w VIRTA transverse: 6min 51 secs T1w VIRTA sagittal: 5 min 52 secs T2w VIRTA sagittal: 3 min 37 secs PDw VIRTA sagittal: 4 min 7 secs	0.88
Yang Q et al., 2017.[30]	Siemens, Verio, 3T, 32ch	Optimize acquisition time	3D T1w VF-TSE	0.53 mm	Whole brain	8min 7 secs	0.94
Zhu C, et al., 2018.[31]	Siemens, Skyra 3T, 20ch	Optimize acquisition time	3D T1w SPACE with compressed sensing	0.5 mm (interpolated)	Whole brain	4 min 31 secs to 6 min 48 secs	1.0
Choi JW, et al., 2018.[40]	Philips, Achieva, 3T, 16ch	Compare sequences	2D PDw, 2D T2w, and 2D T1w TSE with pre-regional saturation pulse; CE-iMSDE-3D TSE MRI	CE-iMSDE-3D TSE MRI: 0.7 mm PDw, T2w, T1w TSE: NR	Imaging range selected by clinician using CTA	PDw: 6 min T2w: 6 min 36 secs T1w: 5 min 40 secs CE-iMSDE-3D MRI: 4 min 50 secs	0.65
Cogswell PM, et al., 2018.[32]	Philips, Achieva, 3T, 32ch	Optimize CSF suppression (DANTE)	3D T1w/PDw TSE with anti-DRIVE with and without DANTE and 3D T2w TSE with DANTE	0.5 mm	NR	4 min 42 secs	0.82
Zhang N, et al., 2018.[39]	Siemens, Verio, 3T, 32ch	Scan-rescan, intra-observer, inter-observer reliability	3D T1 VF-TSE 2D T1 TSE	3D T1w: 0.53 mm 2D T1w: 0.53	3D: Whole brain 2D: vessel segment	3D: 7 min 10sec to 8 min 10 sec 2D: 1 min 37 sec	0.94
Lindenholz A, et al., 2018.[29]	Philips, Achieva, 3T, 8ch	Optimize acquisition time	Compared 7 variants of: 3D T1w VISTA, 3D T1w VIRTA, 3D PDw VISTA Anti-DRIVE used in 3 of 7 variants	Range of acquired resolution: 0.5 mm – 0.6 mm Range of reconstructed resolution: 0.5 mm – 0.6 mm	COW	4 min 39 secs to 8 min 24 secs	0.94

Abbreviations: RSS, reporting summary score; Epub, electronic publication date; ch, channel; min, minutes; secs, seconds; CTA, computed tomography angiography; TSE, turbo spin echo; PD, proton density; VF-TSE, variable flip angle turbo spin-echo; DIR, double inversion recovery; VISTA, volume isotropic turbo spin echo acquisition; SPACE, sampling perfection with Application optimized contrasts using different flip angle evolution; IR, inversion recovery; VIRTA, volumetric isotropically reconstructed turbo spin-echo acquisition; DANTE, delay alternating with nutation for tailored excitation; anti-DRIVE, anti-Driven equilibrium module

*Studies listed in order of online publication date to reflect precision in chronological timeline.

//RRS calculated from modified criteria used in the Nature Reporting Summary.

[**] Multi-site study, MR systems: Magnetom Skyra, 32ch; Magnetom Skyra, 20ch; Magnetom Trio, 12ch; Magnetom Verio, 12ch

[†] Did not report parameter details for high-resolution T2WI.

[//] Reported "to cover the major intracranial vessels as identified on the TOF MRA."

[§§] Reported that a whole-brain MRA was used "for localizing the intracranial arteries."

[††] Reported as "120 coronal slices covering anterior and posterior circulation."

[‡] 7T MR parameters described in Table 3.

[##] Reported as "prescribed to cover the major intracranial vessels."

[§] Tested 3D VF-TSE with anti-DRIVE (pre- and postcontrast), 3D VF-TSE (with TR of 1000 ms and 2 averages), and 3D fast field echo sequence (pre- and postcontrast).

Table 4:

Ultra-high field 7 Tesla Vessel Wall Imaging Publications

Study*	MR Vendor, Magnet Strength, Head coil	Pulse Sequence	Spatial resolution	Anatomic Coverage	Study Aim	Study conclusion
van der Kolk AG, et al., 2011.[49]	Philips, 7T, 16ch	3D T1w MPIR TSE (VF-TSE with CSF suppression MP)	0.8 mm	COW (in vivo)	Develop sequence with goals of improving SNR, nulling CSF, and improving CNR.	Showed feasibility of visualizing vessel walls at 7T in both healthy and diseased intracranial arteries.
van der Kolk AG, et al., 2013.[50]	Philips, 7T, 32ch	3D T1w MPIR TSE (VF-TSE with CSF suppression MP)	0.8 mm	Whole brain (in vivo)	Develop sequence with whole brain coverage with different image contrast weightings	Showed feasibility of a whole-brain multi-sequence vessel wall protocol at 7T.
Majidi S, et al., 2013.[45]	Siemens, 7T, 16ch	3D T1w VF-TSE	0.13 mm	Vessel (ex vivo)	Identify plaque using virtual histology-intravascular ultrasound and compare a subset with 7T MR and histology ex vivo	Virtual histology intravascular ultrasonography and high-resolution MRI at 7T are reliable tools to detect plaque but have limitations with characterizing plaque components.
Kleinloog R, et al., 2014.[46]	Philips, 7T, 32ch	3D T1w MPIR TSE (VF-TSE with CSF suppression MP)	0.8 mm (in vivo); 0.18 mm (ex vivo)	Whole brain (in vivo) and wall biopsy (ex vivo)	Validate in vivo and ex vivo imaging of intracranial aneurysm wall	Unruptured aneurysm wall thickness varies and can be seen as variations in signal intensity with 7T.
van der Kolk AG, et al., 2015.[23]	Philips, 7T, 16ch or 32ch	3D T1w MPIR TSE (VF-TSE with CSF suppression MP)	0.8 mm	COW (in vivo) and whole brain (in vivo)	Examine preferential sites and stability of enhancing intracranial plaque.	Majority of vessel lesions were locationed in the intracranial ICA and M1-M2 MCA segments. At a mean length of 53 days (range: 23–205 days) after initial stroke/TIA presentation, 16.7% of lesions showed change in presence or enhancement characteristics.
Harteveld AA, et al., 2016.[48]	Philips, 7T, 16ch	Driven equilibrium single pulse observation of T1w and T2w, Dual Echo 3D T2 *	0.13 mm	Circle of Willis (ex vivo)	Quantitatively characterize plaque components by obtaining MR signal characteristics and use histologic validation	Different tissue components of plaques can be distinguished with quantitative MR at 7T; T1w imaging is the most promising compared to PD, T2, T2 *.
Blankena R, et al., 2016.[52]	Philips, 7T, 32ch	3D T1w MPIR TSE (VF-TSE with CSF suppression MP)	0.8 mm	Whole brain (in vivo)	Compare 7T and time-resolved 3D PCMR to study aneurysm wall shear stress.	There is an inverse correlation between apparent unruptured aneurysm wall thickness and wall sheer stress.
Viessmann O, et al., 2017.[51]	Siemens, 7T, 32ch	3D T2w VF-TSE versus 3D T2w DANTE prepared VF-TSE	0.5 × 0.5 × 1 mm	NR (in vivo)	Optimize sequence at 7T for sharper wall depiction and contrast	DANTE pre-pulse results in improved CSF-outer lumen wall conspicuity with a trade-off of lower wall-to-lumen contrast.
Zhu C, et al., 2016.[43]	Siemens, 3T, 20ch and 7T, 32ch/	7T: 3D T1w VF-TSE	0.5 mm§	COW or whole brain (in vivo)†	Compare 3D T1 VF-TSE at 3T and 7T of intracranial vessel walls	3D T1 VF-TSE can be used on both 3T and 7T; there is better image quality at 7T.
Harteveld AA, et al., 2017.[44]	Philips, 3T, 8ch and 7T, 32ch/	7T: 3D T1w MPIR-TSE (3D T1w VF-TSE with CSF suppression MP)	0.8 mm (acquired) and 0.49 mm (reconstructed)	7T: Whole Brain (in vivo)	Compare 3T and 7T in elderly asymptomatic population	Vessel wall visibility is equal or significantly better at 7T and most prominent in the proximal anterior cerebral circulation and P2 PCA. The

Study*	MR Vendor, Magnet Strength, Head coil	Pulse Sequence	Spatial resolution	Anatomic Coverage	Study Aim	Study conclusion
						vertebral and basilar arteries were visualized equally well at 3T and 7T.
Harteveld AA, et al., 2017.[16]	Philips, 7T, 32ch	3D T1w MPIR TSE	0.8 mm	Whole brain (in vivo)	Assess vessel wall lesion burden between recent posterior circulation ischemic strokes and healthy controls	Vessel wall lesions in the PCA were more frequently observed in patients than controls. No significant differences in total vessel wall lesion burden in anterior and posterior circulation or in the proportion of enhancing vessel wall lesions between patients and controls.
Harteveld AA, et al., 2018.[47]	Philips, 7T, 16ch	3D T1w gradient echo	0.11 mm (specimen); 0.13 mm (histology)	COW (ex vivo)	Measure vessel wall thickness in ex vivo COW specimens using 7T	MR measurements showed excellent agreement with histology; mean wall thickness varied from 0.45–0.66 mm.

Abbreviations: T, Tesla; Epub, electronic publication date; hr, hour; min, minutes; sec, seconds; COW, circle of Willis; NR, not reported; FOV, field of view; SNR, signal to noise ratio; CNR, contrast to noise ratio; MPIR, magnetization-prepared inversion-recovery; TSE, turbo spin echo; NR, not reported; TIA, transient ischemic attack; VF-TSE, variable flip angle turbo spin echo; CSF, cerebrospinal fluid; MP, magnetization preparation; PCMR, phase-contrast MR; DANTE, delay alternating with nutation for tailored excitation; MCA, middle cerebral artery; PCA, posterior cerebral artery

*Studies listed in order of online publication date to reflect precision in chronological timeline.

†Reports, “prescribed to cover the major intracranial vessels.”

§Acquired resolution not reported; resolution in Table 3 is calculated from parameter details.

/3 Tesla pulse sequence described in Table 2.